

Antisymmetric \mathcal{PT} -photonic structures with balanced positive- and negative-index materials

Li Ge*

*Department of Engineering Science and Physics, College of Staten Island, CUNY, New York 10314, USA
and Department of Electrical Engineering, Princeton University, Princeton, New Jersey 08544, USA*

Hakan E. Türeci

Department of Electrical Engineering, Princeton University, Princeton, New Jersey 08544, USA

(Received 22 August 2012; published 11 November 2013)

We propose a class of synthetic optical materials in which the refractive index satisfies $n(-x) = -n^*(x)$. We term such systems antisymmetric parity-time (\mathcal{APT}) structures. Unlike \mathcal{PT} -symmetric systems, which require balanced gain and loss, i.e., $n(-x) = n^*(x)$, \mathcal{APT} systems consist of balanced positive- and negative-index materials. Despite the seemingly \mathcal{PT} -symmetric optical potential $V(x) \equiv n(x)^2 \omega^2 / c^2$, \mathcal{APT} systems are not invariant under combined \mathcal{PT} operations due to the discontinuity of the spatial derivative of the wave function. We show that \mathcal{APT} systems can display intriguing properties, such as spontaneous phase transition of the scattering matrix, a flat total transmission band, and a continuous lasing spectrum.

DOI: [10.1103/PhysRevA.88.053810](https://doi.org/10.1103/PhysRevA.88.053810)

PACS number(s): 42.25.Bs, 41.20.Jb, 42.55.Ah, 78.67.Pt

I. INTRODUCTION

The pursuit of artificial structures exhibiting unusual electromagnetic properties is a major scientific endeavor. It has led to, for example, the development of photonic crystals for controlling the propagation of electromagnetic waves, utilizing band structures created by Bloch scattering in periodic systems [1]. Another achievement in this pursuit is the design of negative-index materials (NIMs) that are useful for subwavelength imaging [2–5]. In NIMs the refractive index is negative over some frequency range, achieved by engineered electromagnetic resonances in nanostructures. Reduced intrinsic loss and even net gain have been demonstrated in NIMs by gain embedment [6–9].

More recently, there has been growing interest in systems that display parity-time (\mathcal{PT}) symmetry, both in quantum field theory [10–12] and optics [13–15]. By utilizing balanced gain and loss satisfying $n(-x) = n^*(x)$, many intriguing optical phenomena have been predicted and observed, such as double refraction [14], power oscillations [14,16,17], the coexistence of coherent perfect absorption [18,19] and lasing [20–22], and unidirectional transmission resonances [23,24].

In this paper we propose a class of synthetic systems bridging NIMs and \mathcal{PT} -symmetric photonics. Their refractive index is *antisymmetric* under combined \mathcal{PT} operations, i.e., $n(-x) = -n^*(x)$, with balanced positive-index materials (PIMs) and NIMs. In addition, we require that the permeability satisfies $\mu(-x) = -\mu(x)$. The imaginary part of $n(x)$ is symmetric, which can be positive (loss), negative (gain), zero, or any complicated spatial function. We term such synthetic systems antisymmetric parity-time (\mathcal{APT}) structures, and we found that they can display intriguing features, such as spontaneous phase transition of the scattering matrix, a flat total transmission band, and a continuous lasing spectrum.

Below we base our discussion on the scalar Helmholtz equation of the electric field,

$$[\nabla^2 + n(x)^2 (\omega^2 / c^2)]E(x; \omega) = 0, \quad (1)$$

which describes steady-state solutions for transverse electric waves in one-dimensional (1D) and two-dimensional (2D) systems. Henceforth we set the speed of light in vacuum $c = 1$ for convenience. At first glance one may think that all the phenomena found in \mathcal{PT} -symmetric systems would survive since the optical potential $V(x) \equiv n(x)^2 \omega^2$ is still invariant under \mathcal{PT} operation. This is, however, not the case due to the different boundary conditions at PIM and NIM interfaces. Take a 1D \mathcal{APT} heterostructure, for example (see Fig. 1); the electric field itself is still continuous at PIM and NIM interfaces, but its spatial derivation now satisfies [25,26]

$$\frac{1}{\mu_{\text{PIM}}} \frac{\partial E(x; \omega)}{\partial x} \Big|_{x \in \text{PIM}} = \frac{1}{\mu_{\text{NIM}}} \frac{\partial E(x; \omega)}{\partial x} \Big|_{x \in \text{NIM}}, \quad (2)$$

which changes abruptly due to the sign difference of μ_{PIM} and μ_{NIM} . Below we first analyze wave propagation and lasing in 1D \mathcal{APT} heterostructures, followed by a short discussion of pseudo- \mathcal{APT} symmetry for wave propagation in 2D with the paraxial approximation.

II. SCATTERING PHASE TRANSITION

The phase transition of the scattering matrix (S matrix) in a \mathcal{PT} -symmetric system is predicted based on the invariance of the system under combined \mathcal{PT} operations [21]. We would not expect a similar phase transition in \mathcal{APT} systems since

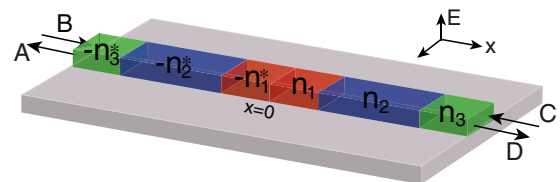


FIG. 1. (Color online) Schematic of a 1D \mathcal{APT} photonic heterostructure, consisting of six layers with $n(-x) = -n^*(x)$.

*li.ge@csi.cuny.edu

flipping the sign of the real part of the refractive index is not related to any symmetry operation of the physical state. However, there do exist some special properties of the transmission coefficient t and the left and right reflection coefficients r_L, r_R in a 1D $\mathcal{AP}T$ heterostructure:

$$r_L = r_R^*, \quad \text{Im}[t] = 0. \quad (3)$$

To understand these properties, we start by noting one observation: By changing the refractive index of each layer in an *arbitrary* photonic heterostructure to its negative complex conjugate and flipping the sign the magnetic permeability, i.e., $n \rightarrow -n^*, \mu \rightarrow -\mu$, the transfer matrix M , defined by

$$\begin{pmatrix} A \\ B \end{pmatrix} = M \begin{pmatrix} C \\ D \end{pmatrix}, \quad (4)$$

becomes its complex conjugate at the same *real* frequency:

$$M(\omega) \rightarrow M^*(\omega), \quad \text{Im}[\omega] = 0. \quad (5)$$

The field amplitudes A, B, C , and D are defined by

$$E(x; \omega) = \begin{cases} Ae^{-in_0\omega(x+L/2)} + Be^{in_0\omega(x+L/2)}, & x < -L/2, \\ Ce^{-in_0\omega(x-L/2)} + De^{in_0\omega(x-L/2)}, & x > L/2 \end{cases}$$

and are illustrated in Fig. 1. Here L is the length of the heterostructure, n_0 is the refractive index of the environment, and we assume the corresponding $\mu_0 = 1$. The proof of (5) is straightforward from the analytical expression of M :

$$M(\omega) = D_0^{-1} [\prod_{j=1}^N m_j] D_0, \quad (6)$$

obtained from the continuity of $E(x; \omega)$ and Eq. (2). The matrices D_0 and m_j are given by

$$D_0 = \begin{pmatrix} 1 & 1 \\ n_0 & -n_0 \end{pmatrix}, \quad (7)$$

$$m_j(\omega) = \begin{pmatrix} \cos(n_j\omega\Delta_j) & i\frac{\mu_j}{n_j} \sin(n_j\omega\Delta_j) \\ i\frac{n_j}{\mu_j} \sin(n_j\omega\Delta_j) & \cos(n_j\omega\Delta_j) \end{pmatrix}, \quad (8)$$

where Δ_j is the width of the i th layer. Under the transformation $n_j \rightarrow -n_j^*, \mu_j \rightarrow -\mu_j$ ($j = 1, \dots, N$), $m_j(\omega)$ becomes $m_j^*(\omega)$ at a *real* frequency and so does $M(\omega)$. Since $M(\omega)$ determines the wave propagation, all related quantities such as r_L, r_R , and t become their complex conjugate under this transformation.

Using (5) and performing a parity operation, we find the following symmetry relation:

$$M_{\mathcal{AP}T}(\omega) = \sigma [M_{\mathcal{AP}T}^{-1}(\omega)]^* \sigma, \quad \sigma = \begin{pmatrix} 0 & 1 \\ 1 & 0 \end{pmatrix}, \quad (9)$$

where $M_{\mathcal{AP}T}(\omega) \equiv \begin{pmatrix} m_{11} & m_{12} \\ m_{21} & m_{22} \end{pmatrix}$ is the transfer matrix of the whole $\mathcal{AP}T$ system. It is then straightforward to show that

$$\text{Im}[m_{11}] = 0, \quad \text{Im}[m_{22}] = 0, \quad m_{12} = -(m_{21})^*. \quad (10)$$

The S matrix defined by

$$\begin{pmatrix} A \\ D \end{pmatrix} = S_{\mathcal{AP}T} \begin{pmatrix} B \\ C \end{pmatrix} \equiv \begin{pmatrix} r_L & t \\ t & r_R \end{pmatrix} \begin{pmatrix} B \\ C \end{pmatrix} \quad (11)$$

can be expressed in terms of $M_{\mathcal{AP}T}$:

$$S_{\mathcal{AP}T}(\omega) = \frac{1}{m_{22}} \begin{pmatrix} m_{12} & 1 \\ 1 & -m_{21} \end{pmatrix}, \quad (12)$$

from which we immediately find (3) using (10).

The phase transition of the S matrix can be inferred from relations (3), which suggest the parametrization of the S matrix by three independent real quantities: $t, a \equiv \text{Re}[r_L]$, and $b \equiv \text{Im}[r_L]$:

$$S = \begin{pmatrix} a + ib & t \\ t & a - ib \end{pmatrix}. \quad (13)$$

We note that this general S matrix is pseudo-Hermitian [27] with respect to σ , i.e., $S^\dagger = \sigma S \sigma^{-1}$. The eigenvalues of the S matrix are given by

$$s_\pm = a \pm \sqrt{t^2 - b^2}, \quad (14)$$

which have two phases, and the phase transitions occur at $t = \pm b$. The scattering eigenstates $\psi_\pm(\omega) = \begin{pmatrix} B_\pm \\ C_\pm \end{pmatrix}$ display a transition simultaneously:

$$p_\pm \equiv \frac{B_\pm}{C_\pm} = \frac{1}{t} [ib \pm \sqrt{t^2 - b^2}]. \quad (15)$$

In one phase ($|t| > |b|$) the intensities of the two incident beams are the same in a scattering eigenstate, i.e., $|p_\pm| = 1$ (see Fig. 2). Thus we refer to this phase as the symmetric scattering phase and the other as the symmetry-broken phase ($|t| < |b|$). In the symmetric phase s_\pm are real, meaning that the symmetric inputs are either amplified or damped equally with no phase added during the scattering process. In the symmetry-broken phase the two scattering eigenstates have the same scattering strength $|s|$ ($s_+ = s_-^*$), but with $|p_+| = |p_-|^{-1}$.

Tuning to the phase-transition points requires either adjusting the gain and loss of the system, adjusting the frequency of the incident beams, or scaling the system size. Given that it is challenging to maintain $\mathcal{AP}T$ (or \mathcal{PT}) symmetry in the first

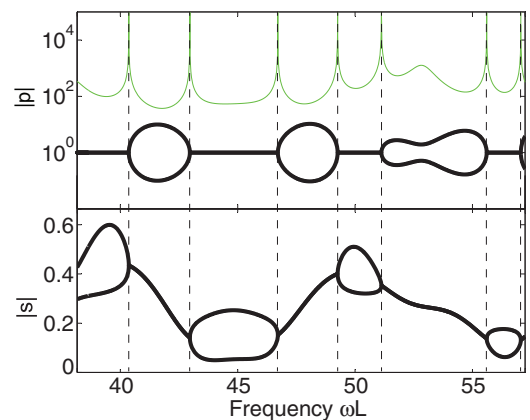


FIG. 2. (Color online) Phase transition of the S matrix in an eight-layer $\mathcal{AP}T$ heterostructure. The widths of the four layers on the right ($x > 0$) are $\Delta_j = 1.2, 0.996, 0.165, 0.531 \mu\text{m}$, and their refractive indices are $\text{Re}[n_j] = 1.3, -2, -1.7, -3$ with $\text{Im}[n(x)] = 0.04$. Thick black solid lines show the transitions of the asymmetry factor $|p|$ and the scattering strength $|s|$. The thin green solid line in the top panel shows $|t^2 - \text{Im}[r_L]^2|^{-1}$, which approaches infinity at the phase-transition points (marked by dashed vertical lines). We take $\mu_{\text{PIM}} = -\mu_{\text{NIM}} = 1$ and the speed of light in vacuum $c = 1$ in all the examples.

two approaches due to material dispersion, the third approach is probably the most practical, i.e., by fabricating multiple scaled heterostructures and fixing the frequency of incident beams at a value that achieves the \mathcal{APT} symmetry.

III. TOTAL TRANSMISSION BAND

The phase transition discussed above is a general property of all 1D \mathcal{APT} systems, independent of whether the system has net gain or loss. By flipping the sign of $\text{Im}[n(x)]$, i.e., changing local gain into loss and vice versa, the system merely undergoes a time reversal, and the scattering phase transitions happen at exactly the same locations. There is one exception, which occurs when the local gain or loss is zero, i.e., $\text{Im}[n(x)] = 0$. In this case an \mathcal{APT} heterostructure is always in the symmetric phase. More striking, relations (3) now become

$$t = 1, \quad r_L = r_R = 0, \tag{16}$$

which is independent of the complexity and size of the heterostructure or the frequency of the incident wave. This phenomenon is robust upon a slight breakdown of the \mathcal{APT} symmetry or in the presence of a small $\text{Im}[n(x)] \neq 0$ [see Fig. 3(a)]. In addition, the total transmission is independent of whether the \mathcal{APT} structure can stand alone or is integrated in a photonic environment, as long as the neighboring elements are the same [see Fig. 3(b)]. A total transmission band then forms if the \mathcal{APT} symmetry can be maintained over a finite-frequency range, and a pulse transmitted within this frequency window will be exactly the same as the initial pulse, with no pulse distortion or shrinkage or expansion. This phenomenon is independent of the propagation direction, in contrast to the one-way invisibility found in \mathcal{PT} -symmetric heterostructures [23].

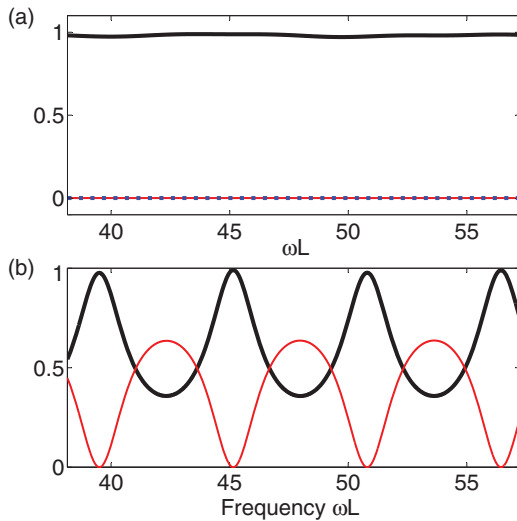


FIG. 3. (Color online) (a) Total transmission band in the \mathcal{APT} heterostructure studied in Fig. 2, but with material loss $\text{Im}[n(x)] = 10^{-4}$. Thick solid black line, thin solid red line, and dotted blue line show $T = |t|^2 \approx 1$, $R = |r_L|^2 \approx |r_R|^2 \approx 0$, and $\text{Arg}[t] \approx 0$, respectively. (b) Same as (a), but with $n_4 = n_{-4} = 3$. The oscillations in R and T have a single period $\Delta\omega L = \pi L/2n_4\Delta_4 = 5.64$, as if the whole structure were a uniform slab formed by the $j = \pm 4$ layers only.

Relations (16) can be treated as a generalization of vanished reflection that happens at the interface of two impedance-matched PIM and NIM materials (see Ref. [2], for example). There is at least one such interface in an \mathcal{APT} system, i.e., at $x = 0$, but multiple reflections occur at other interfaces between two NIMs, two PIMs, and an impedance-mismatched NIM and PIM. One way to prove (16) is from the transfer matrix $M_{\mathcal{APT}}(\omega)$ directly:

$$M_{\mathcal{APT}}(\omega) = D_0^{-1} [\Pi_{j=-N}^N m_j] D_0, \quad j \neq 0. \tag{17}$$

Note that

$$m_{-j}(\omega)m_j(\omega) = \mathbb{1} \tag{18}$$

when n_j is real. Therefore

$$M_{\mathcal{APT}}(\omega) = D_0^{-1} [\Pi_{j=-N, \dots, -2, 2, \dots, N} m_j] D_0 = \dots = \mathbb{1},$$

which implies (16). This derivation indicates not only that relations (16) are due to the existence of matched PIM and NIM layers but also that their spatial arrangement following the \mathcal{APT} symmetry is the key to achieve the phenomenon: it would not occur when the order of the layers is shuffled to break the \mathcal{APT} symmetry since the transfer matrices of individual layers do not commute in general [28]. In Ref. [29] special band gaps ($T = 0$) were reported in photonic crystals with a zero average index, requiring $n_j \Delta_j = -n_{j+1} \Delta_{j+1}$. Relations (16) dictate that these band gaps cannot exist in an \mathcal{APT} heterostructure, even if the latter is periodic. Indeed, we found that these band gaps narrow and disappear completely when the \mathcal{APT} condition is approached (see Fig. 4).

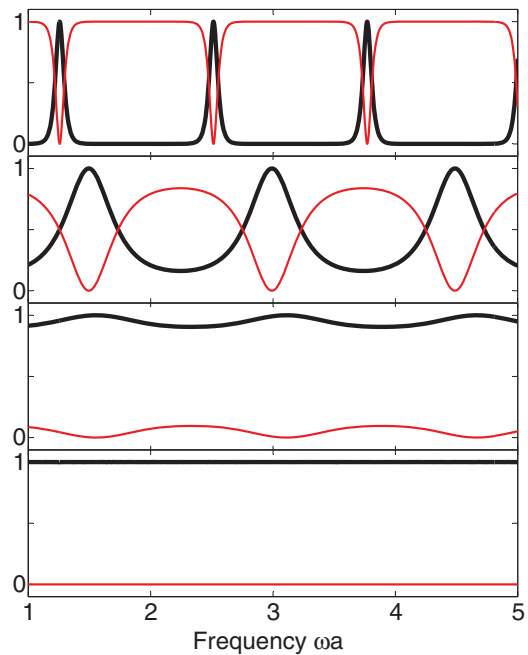


FIG. 4. (Color online) Transition from special band gaps to full-transmission band as the \mathcal{APT} symmetry is approached in a photonic crystal with zero average index. The unit cell has two layers of index, 2 and $-2(1 + \delta)$, and length, $(1 + \delta)a$ and a , and there are 32 unit cells in the photonic crystal. $\delta = 0.25, 0.05, 0.01, 0$ from top to bottom, and thick and thin lines indicate transmittance $T = |t|^2$ and reflectance $R = |r_L|^2 = |r_R|^2$ in each case.

IV. CONTINUOUS LASING SPECTRUM

While loss is an extremely severe detrimental factor in structures containing NIMs, there have been several proposals to overcome it [6–8]. For example, net gain has been demonstrated in optical NIMs by embedding an active medium [9], which opens the possibility of achieving lasing in metamaterials. Lasing modes can be treated as eigenstates of the S matrix with an eigenvalue approaching infinity, which corresponds to a pole of the S matrix [i.e., $m_{22} = 0$ in Eq. (12)] on the real frequency axis. There is usually a discrete set of solutions for the lasing frequency $\omega_L^{(m)}$ and the corresponding threshold $\tau^{(m)} = -\text{Im}[n(x)] > 0$ (assuming a spatially uniform gain). Each lasing mode has its distinct intensity profile, and roughly speaking, the mode order m indicates the number of peaks inside the cavity. To determine $\{\omega_L, \tau\}$ of each mode in a 1D heterostructure, one can, for example, solve the two equations given by the real and imaginary parts of m_{22} . However, Eq. (10) shows that m_{22} is always real for an \mathcal{APT} system, which implies that there exists a continuous region(s) of ω_L in which a ω_L -dependent τ can be found. In other words, an \mathcal{APT} heterostructure has a continuous lasing spectrum, and the mode order m cannot be assigned.

A two-layer \mathcal{APT} structure in the low-frequency regime is shown as an example in Fig. 5. We observe a reduced threshold as the lasing frequency increases and more oscillations gradually appear in the intensity profile, which is symmetric since lasing occurs only in the symmetric phase of the S matrix in an \mathcal{APT} heterostructure. This is because the transfer matrix elements $|m_{12}| = |m_{21}| = 1$ at the pole of the S matrix in an \mathcal{APT} heterostructure, and Eq. (12) implies $|a \pm ib| \rightarrow |t| \rightarrow \infty$ as we approach the pole condition. Therefore $|t| > |b|$ and the S matrix is in the symmetric phase. This observation implies that the continuous lasing spectrum can span more than one frequency window in a complicated \mathcal{APT} system, such as the one shown in Fig. 2. We note that it is the broken-symmetry phase that supports lasing in \mathcal{PT} -symmetric structures instead [21].

If we consider the lasing modes in the corresponding PIM cavity of the same length and $|n|$, we find that its discrete lasing solutions lie exactly on the continuous threshold curve

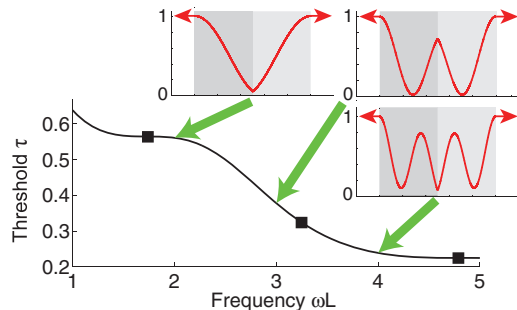


FIG. 5. (Color online) Threshold value $\tau(\omega_L)$ for the continuous lasing spectrum in a two-layer \mathcal{APT} heterostructure. Each layer is 500 nm thick and $n = \pm 2$. Squares indicate the discrete lasing solutions $\omega L = 1.735, 3.245, 4.786$ in a uniform PIM cavity of the same length and $n = 2$. The insets show examples of the intensity profile at $\omega L = 1.5, 3, 4.5$ in the continuous lasing spectrum. Shaded areas indicate the cavity.

of the \mathcal{APT} structure (see Fig. 5). Below we prove this result analytically for the simple two-layer \mathcal{APT} structure discussed above. We note that the threshold $\tau(\omega_L)$ of the continuous lasing spectrum in this case is given by the solution of the following real equation:

$$|\cos \alpha|^2 + \frac{n_r^2 - \tau^2}{n_r^2 + \tau^2} |\sin \alpha|^2 = -\text{Im} \left[\left(n_r - i\tau + \frac{1}{n_r - i\tau} \right) \sin \alpha (\cos \alpha)^* \right], \quad (19)$$

in which n_r is the real part of the refractive index in the PIM, $\alpha \equiv (n_r - i\tau)\omega_L L/2$, and we have taken $\mu_{\text{PIM}} = -\mu_{\text{NIM}} = 1$ for simplicity. In comparison, the threshold and the discrete lasing frequency in a uniform PIM cavity of the same length are determined by the following complex equation:

$$\cos 2\alpha = i \left[\left(n_r - i\tau + \frac{1}{n_r - i\tau} \right) \sin \alpha \cos \alpha \right]. \quad (20)$$

It implies that

$$\tan \alpha = -i(n_r - i\tau), -\frac{i}{n_r - i\tau}, \quad (21)$$

or

$$\text{Re} \left[\frac{\tan \alpha}{(\tan \alpha)^*} \right] = \frac{n_r^2 - \tau^2}{n_r^2 + \tau^2}. \quad (22)$$

By taking the real part of both sides of (20) after multiplying them by $(\cos \alpha)^*/\cos \alpha$, we find

$$|\cos \alpha|^2 + \text{Re} \left[\frac{\tan \alpha}{(\tan \alpha)^*} \right] |\sin \alpha|^2 = -\text{Im} \left[\left(n_r - i\tau + \frac{1}{n_r - i\tau} \right) \sin \alpha (\cos \alpha)^* \right], \quad (23)$$

from which we recover (19) using (22). This finding implies that coherent feedback does occur in an \mathcal{APT} -structure-based laser, even though its spectrum is continuous as in other “white-light” cavities [30–32].

Unlike the total transmission band, the continuous lasing spectrum is singular and breaks down if the \mathcal{APT} symmetry is broken, which can be utilized as a sensitive measure of the quantities of interest that lead to the latter. Here we consider one scenario where the \mathcal{APT} symmetry is broken due to a slight length mismatch. Consider a two-layer cavity of length L similar to that studied in Fig. 5 but with the PIM layer wider than the NIM layer by δ . We found that all lasing modes disappear except the ones at $kL \approx m\pi L/(|n|\delta)$ ($m = 1, 2, \dots$), whose thresholds are about the same as when the \mathcal{APT} symmetry holds ($\delta = 0$). Take $L = 250 \mu\text{m}$, $\delta = 250 \text{nm}$, and $|n| = 2$, for example; the corresponding wavelengths are $\lambda = m^{-1} \mu\text{m}$, which are well separated and make it easy to achieve single-mode lasing. These modes originate from the resonances of the tiny section of length δ , which acts as an external cavity for frequency selection. In this example, the variation of δ (or L) is enhanced by four times in the wavelength of the fundamental mode ($m = 1$) since $\Delta\lambda = 4\Delta\delta/m$, which can be easily measured. As a comparison, the sensitivity to detect δ is reduced by a factor of $L/\delta = 10^3$ using a lasing mode of roughly the same wavelength in a uniform PIM cavity of length L , which also has a much denser spectrum

to analyze. We note that the laser linewidths are comparable in the two systems since the thresholds of the corresponding modes are about the same as discussed.

V. DISCUSSION AND CONCLUSION

So far we have discussed the $\mathcal{AP}\mathcal{T}$ symmetry with balanced PIMs and NIMs. One may attempt to realize a ‘‘pseudo- $\mathcal{AP}\mathcal{T}$ ’’ symmetry using only PIMs (or NIMs), satisfying $n(-x) = -n^*(x)$ but with $\mu(-x) = \mu(x)$. Such a symmetry can be realized, for example, for wave propagation in 2D paraxial geometry [13, 14], with transverse index variation $n(x) = n_0 + \delta n(x)$ satisfying $|\delta n(x)| \ll n_0$ and $\delta n(-x) = -\delta n^*(x)$. Equation (1) for the transverse electric field $E(\tilde{x}, z) = \phi(\tilde{x}, z)e^{ik_0z}$ propagating in the z direction becomes [14]

$$i \frac{\partial \phi(\tilde{x}, z)}{\partial z} + \left[\frac{\partial^2}{\partial \tilde{x}^2} + \delta n(\tilde{x})k_0 \right] \phi(\tilde{x}, z) = 0, \quad (24)$$

where $\tilde{x} \equiv \sqrt{2n_0k_0}x$ and $\phi(\tilde{x}, z)$ is the slowly varying amplitude. The transverse optical potential now is proportional to

$\delta n(\tilde{x})$ instead of n^2 in Eq. (1), and the intriguing phenomena discussed above disappear. The only exception happens when the system becomes equivalent to a conventional \mathcal{PT} -symmetric structure. The latter occurs, for example, if $\delta n(\tilde{x}) = A \sin \tilde{x} + iB \cos \tilde{x}$ ($A, B \in \mathbb{R}$); shifting \tilde{x} by $\pi/2$ transforms $\delta n(\tilde{x})$ to $A \cos \tilde{x} - iB \sin \tilde{x}$, satisfying $n(-\tilde{x}) = n^*(\tilde{x})$.

In summary, we propose a class of synthetic materials which are antisymmetric under combined parity-time operations, i.e., $n(-x) = -n(x)^*$. $\mathcal{AP}\mathcal{T}$ systems demonstrate interesting features such as spontaneous phase transition of the S matrix, a total flat transmission band, and a continuous lasing spectrum. Properties of $\mathcal{AP}\mathcal{T}$ systems in higher dimensions are under investigation and will be reported elsewhere.

ACKNOWLEDGMENTS

We acknowledge A. Douglas Stone, Kostas Makris, Raam Uzdin, and Nimrod Moiseyev for helpful discussions. This research was supported by NSF under Grant No. MIRTHE EEC-0540832 and DARPA Grant No. N66001-11-1-4162.

-
- [1] J. D. Joannopoulos, R. D. Meade, and J. N. Winn, *Photonic Crystals: Molding the Flow of Light* (Princeton University Press, Princeton, NJ, 1995).
- [2] J. B. Pendry, *Phys. Rev. Lett.* **85**, 3966 (2000).
- [3] V. M. Shalaev, W. Cai, U. K. Chettiar, H.-K. Yuan, A. K. Sarychev, V. P. Drachev, and A. V. Kildishev, *Opt. Lett.* **30**, 3356 (2005).
- [4] G. Dolling, M. Wegener, C. M. Soukoulis, and S. Linden, *Opt. Lett.* **32**, 53 (2007).
- [5] J. Valentine, S. Zhang, T. Zentgraf, E. Ulin-Avila, D. A. Genov, G. Bartal, and X. Zhang, *Nature (London)* **455**, 376 (2008).
- [6] V. Shalaev, *Nat. Photonics* **1**, 41 (2007).
- [7] K. Tanaka, E. Plum, J. Y. Ou, T. Uchino, and N. I. Zheludev, *Phys. Rev. Lett.* **105**, 227403 (2010).
- [8] N. Meinzer, M. König, M. Ruther, S. Linden, G. Khitrova, H. M. Gibbs, K. Busch, and M. Wegener, *Appl. Phys. Lett.* **99**, 111104 (2011).
- [9] S. Xiao, V. P. Drachev, A. V. Kildishev, X. Ni, U. K. Chettiar, H.-K. Yuan, and V. M. Shalaev, *Nature (London)* **466**, 735 (2010).
- [10] C. M. Bender and S. Boettcher, *Phys. Rev. Lett.* **80**, 5243 (1998).
- [11] C. M. Bender, S. Boettcher, and P. N. Meisinger, *J. Math. Phys.* **40**, 2201 (1999).
- [12] C. M. Bender, D. C. Brody, and H. F. Jones, *Phys. Rev. Lett.* **89**, 270401 (2002).
- [13] R. El-Ganainy, K. G. Makris, D. N. Christodoulides, and Z. H. Musslimani, *Opt. Lett.* **32**, 2632 (2007).
- [14] K. G. Makris, R. El-Ganainy, D. N. Christodoulides, and Z. H. Musslimani, *Phys. Rev. Lett.* **100**, 103904 (2008).
- [15] A. Regensburger, C. Bersch, M.-A. Miri, G. Onishchukov, D. N. Christodoulides, and U. Peschel, *Nature (London)* **488**, 167 (2012).
- [16] C. E. Rüter, K. G. Makris, R. El-Ganainy, D. N. Christodoulides, M. Segev, and D. Kip, *Nat. Phys.* **6**, 192 (2010).
- [17] M. C. Zheng, D. N. Christodoulides, R. Fleischmann, and T. Kottos, *Phys. Rev. A* **82**, 010103(R) (2010).
- [18] Y. D. Chong, Li Ge, H. Cao, and A. D. Stone, *Phys. Rev. Lett.* **105**, 053901 (2010).
- [19] W. Wan, Y. D. Chong, L. Ge, H. Noh, A. D. Stone, and H. Cao, *Science* **331**, 889 (2011).
- [20] S. Longhi, *Phys. Rev. A* **82**, 031801(R) (2010).
- [21] Y. D. Chong, Li Ge, and A. D. Stone, *Phys. Rev. Lett.* **106**, 093902 (2011).
- [22] H. Schomerus, *Phys. Rev. Lett.* **104**, 233601 (2010).
- [23] Z. Lin, H. Ramezani, T. Eichelkraut, T. Kottos, H. Cao, and D. N. Christodoulides, *Phys. Rev. Lett.* **106**, 213901 (2011).
- [24] L. Ge, Y. D. Chong, and A. D. Stone, *Phys. Rev. A* **85**, 023802 (2012).
- [25] P. Schmidt, I. Grigorenko, and A. F. J. Levi, *J. Opt. Soc. Am. B* **24**, 2791 (2007).
- [26] J. Wiersig, J. Unterhinninghofen, H. Schomerus, U. Peschel, and M. Hentschel, *Phys. Rev. A* **81**, 023809 (2010).
- [27] A. Mostafazadeh, *J. Math. Phys.* **43**, 205 (2002).
- [28] One exception is when all PIMs and all NIMs are identical; see K.-Y. Kim, *Phys. Rev. E* **70**, 047603 (2004).
- [29] J. Li, L. Zhou, C. T. Chan, and P. Sheng, *Phys. Rev. Lett.* **90**, 083901 (2003).
- [30] G. S. Pati, M. Salit, K. Salit, and M. S. Shahriar, *Phys. Rev. Lett.* **99**, 133601 (2007).
- [31] A. Wicht, K. Danzmann, M. Fleischhauer, M. Scully, G. Müller, and R.-H. Rinkleff, *Opt. Commun.* **134**, 431 (1997).
- [32] H. Wu and M. Xiao, *Phys. Rev. A* **77**, 031801(R) (2008).